CLARK
PIGHER

*
**

variables will be specified more precisely below. Several testable new predictions emerge from the treatment presented here:

(1) The x and Q^2 dependences of the quark structure function of the pion $G_{q/\pi}(x,Q^2)$ are obtained explicitly[1] (in the lowest order of $\alpha_s(Q^2)$). In the limit $Q^2 \to \infty$, for $x \geq 0.5$, $G_{q/\pi}(x,Q^2) \propto (1-x)^2$. However, a large non-scaling piece is also present, with a different dependence on x, such that it dominates as $x \to 1$. Thus,

$$G_{\bar{q}/\pi} \to (1-x)^2 + \frac{2}{9}\frac{\langle k_T^2\rangle}{Q^2} \quad . \tag{5}$$

Here $\langle k_T^2\rangle$ is a parameter which effectively includes mass terms as well as the square of the transverse momentum of the annihilating $\bar{q}$ from the pion in $\pi^- N \to \mu\bar{\mu}X$. This prediction has been tested recently in experimental studies[4] of $\pi N \to \mu\bar{\mu}X$, and is consistent with the data.

(2) The z and Q^2 dependences of the quark to pion fragmentation distribution $D_{\pi/q}(z,Q^2)$ are also derived (for $z \geq 0.5$):

$$D_{\pi/q}(z,Q^2) \propto (1-z)^2 + \frac{2}{9}\frac{\langle k_T^2\rangle}{Q^2} \quad . \tag{6}$$

(3) Explicit non-factorizing correlations are predicted in the joint distributions of variables usually considered to be separable. Some of these are:

(a) In deep-inelastic lepton scattering, $lN \to l'\pi X$, the y distribution is shown to depend strongly on z, where $y \equiv Q\cdot p_N/p_\ell\cdot p_N$ and $z \equiv p_\pi\cdot p_N/Q\cdot p_N$. Moreover, the p_T^2 spectrum should depend strongly on z, and important z dependent asymmetries are predicted in the azimuthal angle distribution $d\sigma/d\phi$.

[illegible] the lepton pair transverse momentum [illegible] with the longitudinal momentum fraction [illegible] the lepton pair

$$d\sigma \propto (1+x)^2(1+\cos^2\theta) + \frac{1}{q}\sqrt{\left(\frac{\langle k_T^2\rangle}{Q^2}\right)}(1-x)\cos\phi\sin^2\theta$$

$$+ \frac{1}{q}\frac{\langle k_T^2\rangle}{Q^2}\cos 2\phi\sin^2\theta \qquad (*)$$

At fixed Q^2 ($\equiv M^2_{\mu\mu}$), as x is increased the distribution $d\sigma/d\cos\theta\, d\phi$ changes from that characteristic of a transversely polarized virtual photon to that associated with a longitudinally polarized virtual photon.[1] The x variation of $d\sigma/d\cos\theta$ predicted in Eq. (*) has recently been observed.[4]

(4) Inclusion of effects associated with the pion wave function[5] permits an explicit evaluation of important non-scaling, $1/Q^2$ terms in various cross sections. Although negligible at truly asymptotic energies, the $1/Q^2$ terms are shown here to be especially large in some kinematic regions, notably at large x in the Drell-Yan process and/or large z in deep inelastic scattering, where the leading scaling terms (up to $\log Q^2$ effects) are anomalously small. The "non-scaling" terms are in fact dominant for fixed $Q^2(1-x)$ [or fixed $Q^2(1-z)$] as $Q^2 \to \infty$. Knowledge of the expected form and size of these $1/Q^2$ terms is important for judging how high in Q^2 one must go before data can be used exclusively to test the logarithmic scaling violations[6] associated with gluonic radiative effects in perturbative QCD. Knowledge of the $1/Q^2$ terms also permits QCD fits to data in a region of modest Q^2 where the asymptotic scaling

terms alone are inapplicable. The results may be particularly relevant therefore for reactions in which typical values of Q^2 are not large. The $1/Q^2$ effects obtained here are "higher-twist" effects in QCD, in that they arise from evaluating scattering amplitudes in which more than the minimum number of elementary constituents participate.

(5) Most of the higher-twist effects I discuss in this paper are related to the cross sections σ_L for longitudinally polarized γ^*'s and W's. The explicit forms for the cross sections, for transversely polarized γ^* and W's, as well as for longitudinally polarized γ^* and W's are derived here, with specified relative magnitude. Thus, predictions are provided for the magnitude and kinematic variation of quantities such as σ_L/σ_T.

In the parton model and in the conventional QCD approach to processes such as those in Eqs. (1)-(4), it is customary first to isolate a basic pointlike constituent scattering process. The overall cross section is then expressed as a product of three incoherent probabilistic factors, representing (i) the density of "free" on-shell constituents of the hadrons in the initial state, (ii) the constituent to constituent scattering cross section, and (iii) the probability that the "free" on-shell final constituent "decays" into the observed final state hadrons. The work described here is motivated by a desire to go beyond this simple approach, and to deal with the fact that constituents are not free, but are always bound in hadronic wave functions and are often considerably off-shell.[7] Indeed, at large x and/or at large z, constituents are pulled far off-shell. Accordingly, bound state effects not

normally considered should grow in relevance, and the standard quark-parton model assumption of on-shell constituents becomes increasingly questionable. One of the consequences of on-shell behavior is the dominance of the cross sections associated with transversely polarized virtual photons and W's. When spin-1/2 constituents are far off-shell, however, the longitudinally polarized cross sections may take over, resulting in substantial changes in e.g., observable angular distributions. Data should be examined in an effort to establish this qualitative effect, regardless of the details of the specific model for bound state, off-shell behavior presented here.

The Feynman diagrams I use are the simplest Born diagrams consistent with the desire to include pion structure effects. Higher-order diagrams may be drawn in QCD involving, for example, the radiation of free gluons[6] into the final state. These yield logarithmic ($\log Q^2$) modifications to the results I present, and should be calculated in a later more refined investigation. The physical effects predicted here are amenable to experimental check. Some have already been tested with data on $\pi N \to \mu\bar{\mu}X$.

The process $\pi^- N \to \mu\bar{\mu}X$ is treated in Section III. In Sections IV, V, and VI, I discuss the reactions $\gamma N \to \gamma^* \pi X$, $\pi^- e^- \to \pi X$, and $\pi N \to \pi X$. A brief discussion of $P \to \gamma^* \gamma$ or $\gamma^* \pi^0$ is presented in Section VII, and a short summary can be found in Section VIII.

II. Model for the Pion

The pion is a relativistic many-body system and no pretense is made here that its being described is complete. However, in some well defined regions of phase space, in which the active quark (or anti-quark) constituent is far off-shell, the relevant large momentum behavior of the

wave function can be handled with first order QCD perturbation theory, i.e., by single gluon exchange.[8] This approximation corresponds to the first iteration of the Bethe-Salpeter kernel. Higher iterations[8] provide logarithmic (log Q^2) corrections to the first order results presented here. The specific region of phase space amenable to this treatment is that in which the fractional longitudinal momentum x of the constituent is large, $x \gtrsim 0.5$.

Consider the process sketched in Fig. 1(a) in which a quark constituent is removed from the pion. If this quark carries longitudinal momentum fraction x [light-cone variable] and transverse momentum k_T, relative to the initial pion's direction, then energy momentum conservation may be used to show that

$$p_a^2 = -\frac{k_T^2 + xM_X^2}{(1-x)} + xm_\pi^2 \quad . \tag{8}$$

Here M_X is the mass of the on-shell spectator recoil system, and p_a^2 is the square of the four-vector momentum of the active quark. Equation (8) indicates that if x is large and/or k_T^2 is large, the quark is far off-shell (and spacelike). This large momentum (p_a^2 large) behavior of the pion wave function may then be approximated by single gluon exchange, as sketched in Fig. 1(b). The lines with crosses (×) in Fig. 1(b) are all essentially on-shell, carrying small p^2. The unshaded oval in the diagram on the right-hand side of Fig. 1(b) represents the unspecified small momentum bheavior of the pion wave function, represented here simply by the wave function at the origin, $\psi(\vec{r} = 0)$. In the specific calculations discussed below, I treat the on-shell spectator system, the upper line in Fig. 1(b) as a single on-shell massless quark.

Calculations can be done in which the spectator system is taken instead to be a state of several quarks and gluons (higher Fock state components[8] of the pion wave function). However, such diagrams yield contributions to cross sections which decrease with a greater power of (1-x) [or of (1-z)] than for the leading terms which I retain.

III. The Drell-Yan Process

I discuss first the reaction[1] $\pi^- N \to \mu\bar{\mu}X$. A new result reported here for the first time is a prediction for the azimuthal angle dependence of the cross section. The dominant contribution to $\pi^- N \to \mu\bar{\mu}X$ at large $Q^2 = (p_\mu + p_{\bar{\mu}})^2$ arises from the annihilation $\bar{u}u \to \gamma^* \to \mu\bar{\mu}$, where the antiquark $\bar{u}$ comes from the π^- and u from the nucleon. It is conventional to treat both the incident u and the incident $\bar{u}$ as free, on-shell, massless constituents. Doing so, one obtains immediately the prediction that the angular distribution of the final lepton should follow the form $d\sigma/d\cos\theta \propto (1 + \alpha\cos^2\theta)$, with $\alpha = 1$. This form is characteristic of the coupling of a transversely polarized virtual γ^* to on-shell fermions. Here $\cos\theta = \hat{p}_\mu \cdot \hat{p}_\pi$ is defined in the $\mu\bar{\mu}$ rest frame. For modest transverse momenta of the lepton pair, small deviations from $\alpha = 1$ are expected due to constituent transverse momentum fluctuations.[9]

As the longitudinal momentum fraction x_F of the $\mu\bar{\mu}$ pair is increased towards its kinematic limit, or as $\tau = Q^2/s \to 1$ at fixed x_F, the annihilating antiquark in the pion is forced to carry a large fractional momentum x and is pulled off-shell. Accordingly, bound state and longitudinal polarization effects grow in potential importance. I concentrate on the kinematic region where only the $\bar{u}$ is far off-shell (i.e., $x_F \to 1$). It is sufficient to treat the u quark as nearly free and on-shell. Thus,

the incident nucleon structure is ignored, and I specialize to the reaction $\pi^- q \to \gamma^* q$.

Relying on the discussion in Section II, one may draw the two lowest-order diagrams shown in Fig. 2. Both diagrams in Fig. 2 are required by gauge invariance, although in a physical (axial) gauge, the scaling contributions as $Q^2 \to \infty$ can be identified solely with Fig. 2(a). The incident meson momentum p is partioned equally between the constituent d and $\bar{u}$. If this simplifying approximation is discarded, a modest change occurs in the prediction of the relative size of the transversely polarized and longitudinally polarized components of the final cross section.

The kinematics of the annihilating antiquark are specified with light-cone variables $x_a = (p_a^0 + p_a^3)/(p^0 + p^3)$, and k_{Ta}. With $p_1^2 = m^2$, where m denotes the bare quark mass, energy and momentum conservation may be used to derive

$$p_a^2 = -\frac{\vec{k}_{Ta}^2 + x_a m^2 - x_a(1-x_a)\, m_\pi^2}{(1-x_a)} \quad . \tag{9}$$

As $x_a \to 1$, p_a^2 becomes large and far spacelike. The squared four momentum carried by the gluon in Fig. 2, $k^2 = (p_1 - \tfrac{1}{2}p)^2 = \tfrac{1}{2}(p_a^2 + m^2) - \tfrac{1}{4}m^2$, also becomes large as $x_a \to 1$.

The invariant amplitude corresponding to Fig. 2 is

$$\mathcal{M} \propto \bar{u}(p_+)\, \gamma_\mu\, v(p_-)\, \frac{1}{Q^2}\, \frac{\alpha_s(k^2)}{k^2}\, \psi_\pi(\vec{0})$$

$$\sum_\lambda \bar{u}(p_1)\, \gamma_\alpha\, u_\lambda(p/2)\, \bar{v}_{-\lambda}(p/2) \tag{10}$$

$$\left[-\gamma^\alpha \frac{1}{\not p_a + m} \gamma^\mu + \gamma^\mu \frac{1}{\not p_c - m} \gamma^\alpha\right] u(p_b) \quad .$$

The equality $\sum_\lambda u_\lambda \bar{v}_{-\lambda} = (\not{p} + m)\gamma_5$ specifies that the $\bar{u}d$ bound state is a pseudoscalar. The factor $\psi_\pi(\vec{r} = \vec{0})$ in Eq. (10) represents an integration over the unspecified soft momenta in the pion wave function. Note that in this calculation the quark transverse momentum k_T enters explicitly; it is not an arbitrarily assigned "intrinsic" or "promordial" k_T associated with the $q\bar{q}$ binding in the pion wave function.

For simplicity in what follows, I set $m^2 = 0$ and $m_\pi^2 = 0$, and restrict attention to $k_{Ta}^2 \ll Q^2$. Using the amplitude in Eq. (10), one may compute an explicit expression for the cross section for $\pi^- N \to \mu\bar{\mu}X$.

$$\frac{Q^2\, d\sigma}{dQ^2\, d^2\vec{Q}_T\, dx_L\, d\cos\theta\, d\phi} \propto \int d^2\vec{k}_{Ta}\, dx_a\, d^2\vec{k}_{Tb}\, dx_b\, G_{q/N}(x_b, \vec{k}_{Tb})$$

$$\times \frac{\psi_\pi^2(\vec{0})}{k_{Ta}^4}\left[(1-x_a)^2(1+\cos^2\theta) + \frac{2}{3}\sqrt{\frac{4k_{Ta}^2}{Q^2}}(1-x_a)\cos\theta\sin\theta\cos\phi\right. \tag{11}$$

$$\left. + \frac{1}{9}\frac{k_{Ta}^2}{Q^2}\sin^2\theta\right]\delta^{(2)}(\vec{Q}_T - \vec{k}_{Ta} - \vec{k}_{Tb})\;\delta(x_L - x_a - x_b)\;\delta(Q^2 - x_a x_b s) \quad .$$

The angles θ and ϕ are defined in the $\mu\bar{\mu}$ rest frame. In this frame, the polar ($\hat{z}$) axis is chosen along the direction of the incident pion; $\cos\theta = \hat{p}_\mu \cdot \hat{p}_\pi$. The ($\hat{x}$, $\hat{z}$) reaction plane is the plane defined by $\vec{p}_X$ and $\vec{p}_\pi$, with $\vec{p}_X$ chosen to have a positive component of momentum along $\hat{x}$. The azimuthal angle ϕ is measured with respect to $\hat{x}$. In the approximation in which I am working, $\vec{p}_X = \vec{p}_I$. In practice, some smearing of the angular distribution predicted in Eq. (11) is to be expected from the non-zero nucleon constituent transverse momentum $\vec{k}_{Tb}$ which I have neglected.

In Eq. (11), $G_{q/N}$ is the quark structure function of the nucleon. To obtain Eq. (11), an expansion in inverse powers of Q^2 was performed, and discarded from the square brackets were subasymptotic terms which are of order $Q^{-2}k_{Ta}^2(1-x_a)$ and $Q^{-4}k_{Ta}^4(1-x_a)^{-1}$. The contributions from sea quarks and antiquarks in the meson and nucleon are also ignored in Eq. (11). Equation (11) is accurate in two $Q^2 \to \infty$ limits: (a) the fixed x_a Bjorken limit, and (b) the fixed $W^2 \approx (1-x_a)Q^2/x_a$ limit, with $W^2 >> k_{Ta}^2$. The neglected terms in Eq. (11) must be retained at modest Q^2 for x_a very close to 1 (> 0.95). If <u>scalar</u> instead of <u>vector</u> gluons were used in the amplitude, the only changes in Eq. (11) would be the replacement of the factor (4/9) by the factor 4, and (2/3) by 2. As Eq. (11) stands, it would appear that the cross section diverges as $\vec{k}_{Ta} \to 0$. However, a finite answer should be obtained once finite masses are restored and the full confining properties implied by $\psi(\vec{0})$ are implemented explicitly.

In the Bjorken scaling limit, $Q^2 \to \infty$, at fixed x_a, the valence quark structure function of the pion can be extracted from Eq. (11):

$$G_{\bar{q}/\pi}(x) = \int d^2\vec{k}_T \, G_{\bar{q}/\pi}(x,\vec{k}_T) \propto (1-x)^2 \quad . \qquad (12)$$

The corresponding k_T fall-off produces pairs with a Q_T^{-4} distribution (for $k_{Ta}^2 << Q^2$).

We observe the following additional features of Eq. (11);

(i) We can identify a non-scaling contribution to the structure function. After averaging over $\cos\theta$ and over ϕ, we obtain:

$$G_{\bar{q}/\pi} \to (1-x)^2 + \frac{2}{9}\frac{\langle k_{Ta}^2\rangle}{Q^2} \quad . \qquad (13)$$

The non-scaling contribution is independent of x and will dominate the scaling contribution at fixed $Q^2(1-x)$ as $Q^2 \to \infty$. In our model the relative magnitude of the scaling and non-scaling terms is fixed.

(ii) The non-scaling $1/Q^2$ contribution corresponds to a longitudinal structure function and provides a $\sin^2\theta$ term in the angular distribution $d\sigma/d\cos\theta$, in contrast to the conventional expectation of $(1+\cos^2\theta)$. At fixed Q^2, the $\sin^2\theta$ term dominates in the cross section as $x_F \to 1$. The usual rule that annihilating spin-½ quarks produce transversely polarized photons is modified when off-shell constituents are involved. In our case, the $\bar{\eta}$ is kinematically far off-shell since, as $x_F \to 1$, all of the momentum of the recoil spectator quark must be transferred to the annihilation subprocess. In this situation the spin of the incident meson influences the final angular distribution. In a different language, the bound state effect can be identified with a "high-twist" subprocess, since more than the minimum number of elementary fields is required. Although the large x_F limit is stressed here, the $\sin^2\theta$ term should be important also at fixed x_F when $\tau = Q^2/s \to 1$. In this latter limit, $x_a \to 1$ also.

(iii) A significant non-scaling, non-isotropic azimuthal angle dependence $d\sigma/d\phi$ is predicted in Eq. (11). At fixed Q^2, the coefficient of the $\cos\phi$ term in the square brackets of Eq. (11) grows as $(1-x_a)^{-1}$ relative to the dominant scaling term. In general, one may also expect contributions to $d\sigma/d\phi$ proportional to $\cos 2\phi \sin^2\theta$. However, in this model, the $\cos 2\phi$ terms enter multiplied by factors such as $Q^{-2}k_{Ta}^2(1-x_a)$ and are therefore discarded in the approximation to which I am working.

Identification of the non-scaling piece in the data can be made in several different ways: the x dependence of the cross section at fixed Q^2,s; the angular (θ) dependence at fixed q,Q^2,s; and s dependence at fixed Q^2/s.

Subsequent to these predictions, the change of the angular distribution $d\sigma/d\cos\theta$ with x, predicted in Eq. (11), was observed by the Chicago-Illinois-Princeton collaboration.[4] Their results are shown in Fig. 3. A polarization parameter α may be defined by expressing $d\sigma/d\cos\theta \propto 1+\alpha\cos^2\theta$. In our model, $\alpha = (1-r)/(1+r)$, with

$$r = \frac{4}{9}\,\frac{\langle k_{Ta}^2\rangle}{Q^2(1-x_a)^2} \quad . \tag{14}$$

The expected value of $\langle k_{Ta}^2\rangle$ is somewhat uncertain. In the data, $\langle k_{Ta}^2\rangle$ cannot be identified precisely with the mean of the square of the transverse momentum of the annihilating antiquark. The parameter $\langle k_{Ta}^2\rangle$ in our formulas effectively includes the mass terms which were dropped when we set m_X^2 and $m_\pi^2 = 0$. Accordingly, only a rough estimate of $\langle k_{Ta}^2\rangle$ can be presented. The $\langle p_T^2\rangle$ of a lepton pair is observed to be roughly 2 GeV^2 in $\pi^- N \to \mu\bar{\mu}X$ at 225 GeV/c and in $pN \to \mu\bar{\mu}X$ at 400 GeV/c. Therefore, is not unreasonable to expect that $\langle k_{Ta}^2\rangle \approx 1$ GeV^2. Curves of α versus x_a obtained with this value of $\langle k_{Ta}^2\rangle$ are shown in Fig. 4, along with values of α extracted from the data.[4] The agreement is good.

Owing to the limited range of Q^2 in the data, it has not been possible yet to verify the Q^2 dependence predicted in Eqs. (13) and (14). However, the data may be fitted[4] to the form specified in Eq. (13), and a good fit is obtained with $\langle k_{Ta}^2\rangle = 1.1 \pm 0.2$ GeV^2, in agreement with expectations.

These results should encourage a much more detailed experimental investigation of the large x_F region in $\pi^- N \to \mu\mu X$, with broad angular coverage so that the distribution $d\sigma/d\cos\theta\, d\phi$ can be obtained precisely.

Because of the large non-scaling effect predicted in Eq. (13), one should not expect that data on $\pi N \to \mu\bar{\mu}X$ taken at different energies should all lie on a perfect scaling curve when plotted in the traditional form of $M^4 d^2\sigma/dM^2 dx_F$. Correspondingly, the non-scaling effect in Eq. (13) should be taken into account before an attempt is made to interpret any observed non-scaling behavior purely in terms of $\log Q^2$ QCD effects.

It is important to ask whether large $\sin^2\theta$ contributions to $d\sigma/d\cos\theta$ can be generated by processes different from the hadron structure effect discussed here. At least two effects can be considered and discarded. Purely kinematic constituent transverse momentum fluctuations[9] perturb the $q\bar{q}$ longitudinal axis and thereby produce an effective $\sin^2\theta$ component. However, at small $\vec{Q}_T$ this effect was shown[9] to reduce α only to about $\alpha = 0.8$ in $d\sigma/d\cos\theta = (1+\alpha\cos^2\theta)$ and, more importantly, to be independent of x_F. Second, free gluonic radiation from the initial $\bar{q}$ or q in $\bar{q}q \to \gamma^* g$, as well as the initial gluon process $\bar{q}g \to \gamma^* q$, will lead to a non-vanishing longitudinally polarized cross section, growing in importance with the transverse momentum $\vec{Q}_T$ of the lepton pair.[10] This effect, however, does not grow with x_F at fixed Q_T. Just as for the quantity $R = \sigma_L/\sigma_T$ measured in deep-inelastic processes, the free gluon radiation effects in QCD are most important at small x_F.

The agreement of the data with the structure function presented in Eq. (13) resolves a paradox. Earlier,[11] it had been reported that $G^{exp}_{\bar{q}/\pi} \propto (1-x)$. However, experimental observation of an effective $(1-x)^1$

behavior of the quark structure function of the pion is incompatible with general crossing arguments for Born diagrams which mandate only even powers of $(1-x)$ as $x \to 1$ when a fermion is extracted from a meson.[12] The linear behavior $(1-x)$ would be expected for spinless quarks. On the other hand, the spin-½ nature of the constituents seemed well established by the observation in the same experiment of a decay angular distribution (averaged over all x_F) of $1+\alpha\cos^2\theta$ with $\alpha \simeq 1$. Our analysis provides a resolution of this apparent paradox. We suggest that the observed $(1-x)^1$ behavior is an approximation to our Eq. (13), in which only even powers of $(1-x)$ appear. The critical test of this assertion is the identification of the predicted $\sin^2\theta$ behavior of the decay angular distribution at large x_F.

In baryon (or antibaryon) induced reactions, $BB \to \mu\bar{\mu}X$, the $1+\cos^2\theta$ behavior characteristic of spin-½ systems is maintained as $x \to 1$, in spite of the fact that an annihilating constituent is again far off-shell. It would be valuable to verify this expectation experimentally. Non-scaling longitudinal contributions should arise near $x = 2/3$ if we take into account the subprocess $(qq)+\bar{q} \to q+\gamma^*$ with a bosonic diquark system.[13,14] These effects may be related to the anomalous value of σ_L/σ_T observed in deep inelastic electron scattering at moderate values of Q^2.

We emphasize that the dominance of the longitudinally polarized cross section ($\propto \sin^2\theta$) as $x_F \to 1$ in $\pi N \to \gamma^* X$ is a direct indication that in this limit the annihilating antiquark carries the signature of its origins in a spin zero meson. The $\sin^2\theta/Q^2$ term is a higher-twist effect in QCD, in that more than the minimum twist $q\bar{q} \to \gamma^*$ configuration

is required to produce it. Observation of the $\sin^2\vartheta/Q^2$ term in the data is the first direct identification of a higher-twist effect in an inclusive reaction. The importance of this higher-twist effect in $\pi^- N \to \mu\bar{\mu}X$, for values of Q^2 as large as ~ 20 GeV^2, suggests that higher-twist effects should be examined carefully in all other high energy processes as well.

IV. Single Pion Production in Deep-Inelastic Scattering

I consider next the process $\ell N \to \ell'\pi X$, as sketched in Fig. 5(a). Here it is convenient to let the momentum of the exchanged γ^* (or W in the case of νN) define the positive longitudinal ($\hat{z}$) direction:

$$Q = p_\ell - p_{\ell'}, \tag{15}$$

The final pion has transverse momentum $\vec{p}_T$ relative to the direction of Q, and it carries the fraction z of the energy of the initial exchanged quantum. In terms of four-vectors, $z = p_\pi \cdot p_N / Q \cdot p_N$. In the lab frame $z = E_\pi/\nu$. The initial quark from the initial nucleon in Fig. 5(a) is assumed to be on-shell and to carry longitudinal momentum fraction x of the nucleon's momentum, and no transverse momentum. The intermediate quark p_a in the subprocess $Q + xp_N \to \pi + q$ is then off-shell and timelike, with

$$p_a^2 = \frac{p_T^2}{z(1-z)} \quad . \tag{16}$$

Note that as $z \to 1$, $p_a^2 \to \infty$. Accordingly, important off-shell effects and deviations from the usual quark-parton model expectations, including longitudinal polarization of the exchanged γ^* or W, may be expected in the limit of large z. The quark and pion masses have been neglected in

the derivation of Eq. (16). Note that here $x = (p_n^2 - Q^2)/2Q \cdot p_N$, and $Q^2 < 0$.

For large z ($\gtrsim 0.5$) we may use the arguments developed in Section II to represent the process $q \to \pi X$ by the diagram indicated in Fig. 5(b). The gauge-invariant set of diagrams for the process $\ell N \to \ell' \pi X$ is presented in Fig. 6. To describe the lepton kinematics, it is conventional to use the variable $y = Q \cdot p_N / p_\ell \cdot p_N$. The initial and final lepton momenta are chosen to lie in the $(\hat{x},\hat{z})$ plane, both having positive $\hat{x}$ components of momentum. The angle ϕ is the azimuthal angle of p_T relative to this $\hat{x}$ direction.

Evaluating the Feynman diagrams in Fig. 6 explicitly, for $\mu N \to \mu' \pi X$ or for $eN \to e' \pi X$, I obtain the cross section (for $p_T^2 \ll |Q^2|$, and large z):

$$\frac{z\, d\sigma}{dz\, dy\, d\phi\, dp_T^2} \propto \int G_{q/N}(x)\, dx\, \frac{1}{y\, p_T^4 Q^2}$$

$$\left\{ (1-z)^2 \left[\frac{1+(1-y)^2}{2} \right] + \frac{2}{3}(1-z)\left[1+(1-y)\right](1-y)^{1/2} \cos\phi \left(\frac{p_T^2}{-Q^2} \right)^{1/2} + \frac{4}{9}(1-y)\frac{p_T^2}{(-Q^2)} \right\} \qquad (17a)$$

Here $Q^2 < 0$. Terms have been dropped which are down in magnitude by powers of $(1-z)$ or of p_T^2/Q^2 relative to those in the curly brackets in Eq. (17a). Thus Eq. (17a) is accurate in two $|Q^2| \to \infty$ limits: (a) the fixed z, $Q^2 \to \infty$ "Bjorken limit", and (b) the fixed $(1-z)$ $|Q^2|$ limit, with $(1-z)\,|Q^2| \gg p_T^2$. The omitted terms must be restored at very small Q^2 or for z very near 1. The cross section also contains terms proportional to $\cos 2\phi$; however, the coefficients of these terms are of order

$(1-z)\ p_T^2/Q^2$. They are therefore negligible in relation to the terms I retain, which are proportional to $(1-z)^2$, $(1-z)(p_T^2/-Q^2)^{\frac{1}{2}}$, or p_T^2/Q^2.

For $\nu N \to \mu^- \pi^+ X$, the expression in curly brackets in Eq. (17a) is replaced by

$$\left\{(1-z)^2 + \frac{2}{3}\ (1-z)(1-y)^{\frac{1}{2}} \cos\phi \left(\frac{4p_T^2}{-Q^2}\right)^{\frac{1}{2}} + \frac{4}{9}\ (1-y)\left(\frac{p_T^2}{-Q^2}\right)\right\} . \quad (17b)$$

For $\bar{\nu}N \to \mu^+ \pi^- X$, the term in the curly brackets in Eq. (17a) becomes

$$\left\{(1-y)^2(1-z)^2 + \frac{2}{3}\ (1-z)(1-y)^{3/2} \cos\phi \left(\frac{4p_T^2}{-Q^2}\right)^{\frac{1}{2}} + \frac{4}{9}\ (1-y)\left(\frac{p_T^2}{-Q^2}\right)\right\} . \quad (17c)$$

A wealth of predictions is embodied in Eqs. (17) involving the correlated behavior of all the variables z, y, p_T^2, and ϕ.

(i) In the fixed z, $Q^2 \to \infty$ limit, the cross sections in Eqs. (17) attain the scale invariant form expected in the usual parton model, with $d\sigma/dy \propto [1 + (1-y)^2]$ for $\mu N \to \mu' \pi X$, $d\sigma/dy \propto (1-y)^2$ for $\bar{\nu}N \to \mu^+ \pi X$, and $d\sigma/dy$ independent of y for $\nu N \to \mu^- \pi X$. However, important deviations are predicted at finite Q^2, as described below.

(ii) According to Eqs. (17), for $\ell N \to \ell' \pi X$, the distribution $d\sigma/dp_T^2$ is expected to decrease as p_T^{-4} (for $p_T^2 << Q^2$), except at large z, where a less rapid p_T^{-2} behavior sets in. Thus, the mean $\langle p_T^2 \rangle$ should grow at large z, a "seagull" type of effect. This "jet broadening" phenomenon is distinct from that associated with gluonic radiation diagrams.[6] The two effects may be distinguished in the data by their different dependences on z and Q^2.

(iii) In the limit $Q^2 \to \infty$, the y and z dependences in Eqs. (17) are separable. In this limit, an asymptotic quark to pion fragmentation function may be extracted from Eqs. (17). For $z > 0.5$ and $Q^2 \to \infty$,

$$D_{\pi/q}(z, Q^2) \to (1-z)^2 \quad , \tag{18}$$

Moreover, after averaging Eq. (17b) over y, ϕ, and p_T^2, one may identify a significant non-scaling term in $D_{\pi/q}(z,Q^2)$:

$$D_{\pi/q}(z,Q^2) \propto (1-z)^2 + \frac{2}{9} \frac{\langle p_T^2 \rangle}{-Q^2} \quad . \tag{19}$$

The extra non-scaling term in Eq. (19) is independent of z, and is especially relevant at large z where the scaling term vanishes rapidly. The form of Eq. (19) is similar to the popular phenomenological form proposed by Feynman and Field,[15] except for the important difference here that the constant term (independent of z) falls as $1/Q^2$. A comparison of Eqs. (12) and (18) shows that (for $x > 0.5$)

$$G_{\bar{q}/\pi}(x, |Q^2|) \propto D_{\pi/q}(x, |Q^2|) \quad ,$$

as expected from general arguments.[12] Upon multiplying Eq. (19) by z^{N-1} and integrating over z, one may obtain a prediction for the Q^2 dependence of fragmentation moments. However, caution is in order since Eq. (19) is valid only for $z \gtrsim 0.5$.

(iv) For modest values of Q^2 or for large z, a significant non-factorizing, non-scaling term is present in Eqs. (17). Averaging over ϕ, I obtain:

For $ep \to e'\pi X$ or $\mu p \to \mu'\pi X$,

$$\sigma(z,y,Q^2) \propto (1-z)^2\left[\frac{1+(1-y)^2}{2}\right] + \frac{4}{9}(1-y)\left(\frac{p_T^2}{-Q^2}\right) \quad . \qquad (20a)$$

For $\nu p \to \mu^-\pi^+X$,

$$\sigma(z,y,Q^2) \propto (1-z)^2 + \frac{4}{9}(1-y)\left(\frac{p_T^2}{-Q^2}\right) \quad . \qquad (20b)$$

For $\bar{\nu}p \to \mu^+\pi^-X$,

$$\sigma(z,y,Q^2) \propto (1-z)^2(1-y)^2 + \frac{4}{9}(1-y)\left(\frac{p_T^2}{-Q^2}\right) \quad . \qquad (20c)$$

These expressions imply that at large z, the distributions in y should be very different from "normal." Likewise, selections on y can lead to considerably different expectations for the distribution in z. The term proportional to $\frac{4}{9}(1-y)(p_T^2/-Q^2)$ is the analog of the $\frac{4}{9}\sin^2\theta\,(k_T^2/Q^2)$ term found in $\pi^-N \to \mu\bar{\mu}X$, and corresponds to a longitudinally polarized γ^* or W. It would be valuable to ascertain whether its contribution is as significant in deep-inelastic scattering as it appears to be in $\pi^-N \to \mu\bar{\mu}X$.

(v) Note that in the limit $z \to 1$ at fixed Q^2, or in the limit $Q^2 \to \infty$ with $Q^2(1-z)$ fixed, the terms which dominate in Eqs. (17) are the unusual, higher-twist terms $\propto (1-y)$. Thus in either of these limits, the cross section $d\sigma/dy$ is predicted to have an unusual dependence, varying as $(1-y)$ for all three processes: $\mu N \to \mu'\pi X$, $\nu N \to \mu^-\pi^+X$, and $\bar{\nu}N \to \mu^+\pi^-X$.

(vi) The ϕ distributions in Eqs. (17) are particularly interesting. Ignoring for the moment the terms proportional to p_T^2/Q^2, I find

$$\langle\cos\phi\rangle_{eN} = \left(\frac{4p_T^2}{-Q^2}\right)^{\frac{1}{2}} \frac{1}{(1-z)} \frac{(2-y)(1-y)^{\frac{1}{2}}}{3[1+(1-y)^2]} \quad ; \qquad (21a)$$

$$\langle\cos\phi\rangle_{\nu N} = \left(\frac{4p_T^2}{-Q^2}\right)^{\frac{1}{2}} \frac{(1-y)^{\frac{1}{2}}}{3(1-z)} \quad ; \qquad (21b)$$

$$\langle\cos\phi\rangle_{\bar{\nu}N} = \left(\frac{4p_T^2}{-Q^2}\right)^{\frac{1}{2}} \frac{1}{3(1-z)(1-y)^{\frac{1}{2}}} \quad . \qquad (21c)$$

In all cases, the asymmetry is positive. The y and $[p_T^2/-Q^2]^{\frac{1}{2}}$ dependences in Eqs. (21) may be expected on general kinematic grounds. The new feature in these equations is the dependence on (1-z). All show an increase of $\langle\cos\phi\rangle \propto 1/(1-z)$ as z increases. For z very near 1, the neglected $p_T^2/-Q^2$ term in Eqs. (17) should be retained; the growth of $\langle\cos\phi\rangle$ will then level off, and $\langle\cos\phi\rangle = 0$ at $z = 1$.

The z dependences of Eqs. (21) may be contrasted with the behavior $(1-z)^{\frac{1}{2}}$ expected from QCD gluonic radiation[16] and with the z independent behavior provided by pure kinematics.[17] The $(1-z)^{-1}$ asymmetry calculated here is a manifestation of the higher-twist QCD contribution resulting from including explicitly effects associated with the pion bound state. The complete behavior of $d\sigma/d\phi$ may be predicted only after inclusion of the QCD gluonic radiation effects and the kinematic effects associated with transverse momentum fluctuations of the initial quark. Since the gluonic radiation[16] and the kinematic effects[17] appear to provide negative values of $\langle\cos\phi\rangle$, the effects predicted in Eqs. (21) will be somewhat washed out. The essential new feature of Eqs. (21) is the growth proportional to $1/(1-z)$.

The asymmetry $\langle\cos 2\phi\rangle$ may also be computed. However, in the approach described here, I find

$$\langle\cos\,2\phi\rangle \propto \frac{P_T^2}{-Q^2(1-z)} \quad ,$$

which is negligible in the limit in which I am working.

(vii) In the computations described here, only those hadron structure effects associated with the final pion are considered in $\ell N \to \ell'\pi X$. In a more complete investigation, off-shell effects associated with the initial quark from the incident nucleon should also be treated. These will be especially relevant for $x > 0.5$ and should lead to the prediction of correlations in the x and z dependences of the cross section. A thorough treatment of the low Q^2 domain in $\ell N \to \ell'\pi X$ should also include the possibility of the γ^* or W scattering from the diquark subcomponents of the nucleon.[13,14]

Although evidence[15] is present already in the data for a non-vanishing component of $D_{\pi/q}(z,Q^2)$ as $z \to 1$, detailed verification of Eq. (19) and a determination of the magnitude of the non-scaling term may be difficult because observed pions are also produced "indirectly" from resonance decay: $q \to RX$, $R \to \pi X'$. The fragmentation function in Eq. (19) and other properties of Eqs. (17) apply only to the direct $q \to \pi X$ component. (This type of complication is not present in $\pi^- N \to \mu\bar{\mu}X$, where the $\pi \to \bar{q}X$ structure function is determined.) Neutrino reactions, $\nu N \to \mu^- \pi^+ X$, would seem to offer the best opportunity to examine $D_{\pi^+/q}(z,Q^2)$ clearly, and to test the other spin-related predictions (correlations, asymmetries) listed above, with a minimum of background from indirect sources, such as $q \to \rho^0 \to \pi^+\pi^-$. In an attempt

to remove backgrounds, it might be useful to compare the predictions with data on the difference of the π^+ and π^- yields.

V. e^+e^- Annihilation

The process $e^+e^- \to \pi X$ may be handled by the same methods discussed above. The relevant gauge-invariant set of Feynman diagrams is shown in Fig. 7. After evaluating the amplitudes explicity, for $Q^2 \gg k_T^2$ and for large z, I derive the cross section

$$\frac{d\sigma}{dk_T^2\, dz\, d\cos\theta} \propto \frac{1}{k_T^4}\left[(1-z)^2(1+\cos^2\theta) + \frac{4}{9}\frac{k_T^2}{Q^2}\sin^2\theta\right] \qquad (22)$$

Here $z = 2p_\pi \cdot Q/Q^2$, $Q^2 > 0$, and k_T is the transverse momentum of the π with respect to the direction of the decaying quark p_a in Fig. 7(a); $\cos\theta = \hat{p}_\pi \cdot \hat{p}_e$ in the overall e^+e^- center of mass frame. The first term in Eq. (22) displays the expected jet axis distribution $(1+\cos^2\theta)$ characteristic of a transversely polarized intermediate γ^*. In the limit $Q^2 \to \infty$, one may again identify a quark to pion decay distribution $D_{\pi/q}(z,Q^2) \propto (1-z)^2$, for $z > 0.5$. However, for fixed Q^2 as $z \to 1$ or for fixed $Q^2(1-z)$ as $Q^2 \to \infty$, the second, non-scaling term in Eq. (22) dominates the cross section.[3] The second term is proportional to $\sin^2\theta$, characteristic of a longitudinally polarized intermediate γ^*.

At large enough z, the exclusive process $e^+e^- \to \pi\pi$ will provide an important contribution to $d\sigma/d\cos\theta$. The cross section for this exclusive process is necessarily of the form $d\sigma/d\cos\theta \propto \sin^2\theta$, and Eq. (22) therefore is endowed with the correct exclusive limit. However, Eq. (22) is derived from a purely inclusive amplitude for $e^+e^- \to \pi X$ with no imposition in the calculation that $X \to \pi$ as $z \to 1$.

Rewriting Eq. (22) in the form $d\sigma/d\cos\theta \propto [1 + \alpha\cos^2\theta]$, I obtain

$$\alpha = \frac{1 - r}{1 + r} \quad . \tag{23}$$

with $r = (4/9)\langle k_T^2\rangle/[Q^2(1-z)^2]$. The form of this result is identical to that derived earlier for the angular distribution of the final μ in $\pi^- N \to \mu\bar{\mu}X$. For comparison with data, one must bear in mind again that the parameter $\langle k_T^2\rangle$ effectively includes mass terms which were neglected in the calculation ($m_q = 0$, $m_\pi = 0$, $m_{\bar{q}} = 0$). Therefore, $\langle k_T^2\rangle$ may not be equated directly to the measured values of the mean of the square of the momentum transverse to a specified jet axis.[18] A second difficulty must be faced. The Eqs. (22) and (23) apply only to pions produced directly from quark fragmentation $q \to \pi X$, whereas a substantial fraction of the observed pions probably arises through the sequence $q \to RX$, where R is a resonance; $R \to \pi R'$. The resonance terms do not necessarily provide both $\sin^2\theta$ and $(1 + \cos^2\theta)$ contributions in the same ratio and with the same z dependence as shown in Eq. (22).

Bearing in mind the doubts expressed above, one may note nevertheless that Eq. (22) predicts that the distribution $d\sigma/dk_T^2$ should flatten as z increases, with $\langle k_T^2\rangle$ growing with z. This trend is observed in the data.[18] For [illegible], data[13] from $e^+e^- \to hX$ suggest that $\langle k_T^2\rangle \simeq 0.25$ GeV^2. Using this value, I obtain the curves of α vs. z shown in Fig. 8. The annihilation process $e^+e^- \to \pi X$ is therefore a third reaction in which to attempt to identify and measure the strength of the non-scaling higher twist effects related to the [illegible] behavior of the pion wave function.

VI. High p_T Single Pion Production

The diagram in Fig. 9 shows one of the members of the gauge-invariant set of graphs for $qq \to \pi qq$ relevant for the description of $h_1h_2 \to \pi X$ at large transverse momentum p_T. Evaluating these diagrams explicitly, in the same fashion as discussed above, one may obtain the cross section

$$\frac{E d\sigma}{d^3\vec{p}} \propto \frac{1}{p_T^4}\left[(1-x_T)^2 + \frac{c}{p_T^2}(1-x_T)^0\right] \quad . \tag{24}$$

Here p_T is the transverse momentum of the final π measured with respect to the incident hadron h_1h_2 direction, and $x_T = 2p_T/\sqrt{s}$. Obvious in Eq. (24) is the usual asymptotic decrease $\propto p_T^{-4}$, multiplied by the same quark to pion decay function $\propto (1-x_T)^2$ deduced in $e^+e^- \to \pi X$ and in $\ell N \to \ell'\pi X$. The second term in Eq. (24) is smaller by a factor p_T^{-2}, but it is enhanced relative to the first by the factor $(1-x_T)^{-2}$. The well known "trigger bias" effect[19] implies that observed pions are those with maximum x_T. Thus the second "non-scaling" term in Eq. (24) should have considerable practical importance in studies of $h_1h_2 \to \pi X$ at large p_T, providing a substantial p_T^{-6} component of the cross section. Full details of this study of high p_T production will be published elsewhere.

VII. Diquark in the Nucleon

I want to mention briefly a recent discussion[14] of the x and Q^2 dependences of the ratio $R = \sigma_L/\sigma_T$ in deep inelastic electroproduction $ep \to e'X$. Contributions to σ_L may arise from at least three sources: (i) constituent transverse momentum fluctuations, (ii) QCD free gluon radiation diagrams, and (iii) higher-twist hadronic structure terms

analogous to those discussed earlier in this report. The x and Q² dependences of these three contributions are different, with the higher twist effects being particularly significant at large x, where the QCD gluonic radiation terms are negligible.[6]

In order to compute hadron structure effects associated with the nucleon, an explicit model for the nucleon bound state must be devised, similar to that discussed in Section VI for the pion. The dominant contribution in the large x limit is provided by the three quark component sketched in Fig. 10(a). An approximate treatment of this three quark system will be presented here.

Two of the three quarks in Fig. 10(a) may always be paired in a diquark (qq) system with integer spin.[13,20] It is then interesting to consider the coupling of a virtual photon either to the bachelor, unpaired spin-½ quark as in Fig. 10(b) or to the diquark as in Fig. 10(c). Treating the diquark for the moment as a massless elementary spin-zero system, one may quickly devise a gauge invariant set of scattering amplitudes corresponding to Figs. 10(b) and 10(c), with one gluon exchange used to represent the far off-shell behavior of either the quark, or of the diquark, in the large x limit. This treatment parallels that described for other processes in earlier sections of this report.

For the case sketched in Fig. 10(b), I obtain a cross section which is purely of transverse polarization character, even in the limit $x \to 1$ where the spin-½ constituent is far off-shell. From Fig. 10(c), I obtain contributions to both σ_L and σ_T:

$$\sigma_L = A_d(1-x)^2 \quad ; \tag{25a}$$

$$\sigma_T = \frac{1}{2} A_d \frac{\langle k_T^2 \rangle}{Q^2} \quad , \qquad (25b)$$

Because the scattering in Fig. 10(c) occurs from an integer spin system, the longitudinal cross section σ_L is dominant asymptotically as $Q^2 \to \infty$. However, the transverse term σ_T takes over as $x \to 1$ for fixed Q^2. In Eq. (25b), $\langle k_T^2 \rangle$ is the mean squared transverse momentum of the diquark system in the nucleon (again, masses are neglected). Summing the contributions from Figs. 10(b) and 10(c), one may obtain cross sections for $ep \to e'X$:

$$\sigma_T = A(x)(1-x)^3 + \frac{1}{2} A_d \frac{\langle k_T^2 \rangle}{Q^2} F^2(Q^2) \quad , \qquad (26a)$$

and

$$\sigma_L = A_d (1-x)^2 F^2(Q^2) \quad . \qquad (26b)$$

The diquark form factor $F(Q^2)$ represents the fact that the diquark is a composite (qq) system.[13] It is parametrized as

$$F(Q^2) = (d^2 + Q^2)^{-1} \quad , \qquad (27)$$

with $d^2 = 2$ GeV^2. In Eq. (26), the function $A(x)$ is slowly varying, and the constant A_d may be related to the probability to find a diquark in the nucleon at some specified x and Q^2. From the parameters listed in Ref. 14, it appears that for $Q^2 = 2$ GeV^2 and $x = 0.4$, the probabilities are equal for scattering from the free quark and from the diquark.

The ratio $R = \sigma_L/\sigma_T$ obtained from Eqs. (26) obviously increases with x at fixed Q^2 over most of the range of x, before falling to zero at $x = 1$. To fix the free parameters in the equations, data on the Q^2

and x dependence of $F_2(x, Q^2)$ ... $\sigma_L + \sigma_T$ were fitted for x > 0.5 and Q^2 > 3 GeV^2. The resulting curves for R are compared with available data[21] in Fig. 11. The data appear to be more constant in x and Q^2 than the theoretical expectations. Improvement in the low x region may be expected from the inclusion of QCD gluonic radiation contributions.[6] However, what is important to note in Fig. 11 is that the magnitude of R at high x and low Q^2 can be reproduced adequately with this model of a higher-twist contribution, represented here by diquark substructure. Further experimental checks of the diquark idea are proposed in Ref. 14.

VIII. Summary

Several testable new predictions may be obtained if the scope of perturbative QCD calculations is enlarged so as to include aspects of the binding of constituents into (color singlet) hadrons. Since these effects are related to hadronic structure and involve mass or transverse momentum scales, it is not unexpected that they yield non-scaling contributions to cross sections which are reduced by a power of Q^2 from the asymptotically dominant scale invariant terms. However, as shown here, the new higher-twist, structure-related effects have a different dependence at fixed Q^2 on such variables as x and z. Accordingly, they may, and in some cases do, overwhelm the leading term in predictions in specified kinematic regions. The new effects may also lead to sizeable longitudinal polarization, absent from an approach in which constituents are treated as free and on shell. Correlations are also predicted in the behavior of cross sections as a function of kinematic variables including x, z, y, t, and p_T^2.

In the conventional QCD approach to hard scattering processes, where the initial and final constituents are treated as free partons, scaling violations (the dependence of cross sections on $\log Q^2$) arise from higher order processes in which gluons are emitted. Nothing in this report is in conflict with this conventional QCD approach. Rather, an attempt is made here to emphasize different physics. In a complete treatment, both hadron structure and gluonic radiation effects should be included. Confusion or conflict may arise, nevertheless, in the interpretation of phenomena observed experimentally. Data over a limited range in Q^2 cannot be used with certainty to distinguish a logarithmic fall with Q^2 from the inverse power dependence expected from higher-twist effects.[22] Likewise, it may be inappropriate to identify various non-factorizing effects, or correlations in the data, with next to leading, higher order QCD corrections without first examining the relevance of hadronic-structure effects.

From a theoretical point of view, higher-twist terms must be present. The data from $\pi^- p \to \mu\bar{\mu}X$, discussed in Section III, and perhaps the behavior of R show that their contributions are significant. In those reactions where typical values of Q^2 tend to be small, the relevance of higher-twist effects should be particularly enhanced. In an effort to identify and isolate these hadronic-structure effects, effective use may be made of their characteristic x and z dependences, their spin/polarization properties, and the other correlations discussed in this report.

ACKNOWLEDGMENTS

In the course of the investigations reported here, I have been [illegible] with colleagues at SLAC, especially Stanley Brodsky, Dick Blankenbecler, and Larry Abbott with whom I have worked on some of the topics treated in this report. I am [illegible] for [illegible] and helpful comments on an earlier draft of this paper.

REFERENCES

1. E. L. Berger and S. J. Brodsky, Phys. Rev. Lett. 42, 940 (1979), and references therein. The prediction that the scaling component of the pion structure function should behave as $(1-x)^2$ was derived previously by Z. Ezawa, Ref. 2, and the presence of a non-scaling term is discussed by G. Farrar and D. Jackson, Ref. 3.

2. Z. F. Ezawa, Nuovo Cimento 23A, 271 (1974).

3. G. R. Farrar and D. R. Jackson, Phys. Rev. Lett. 35, 1416 (1975); A. I. Vainshtain and V. I. Zakharov, Phys. Lett. 72B, 368 (1978).

4. Chicago-Princeton Collaboration, K. J. Anderson et al., Report Number EFI 79-34 (June, 1979).

5. S. J. Brodsky and G. R. Farrar, Phys. Rev. D11, 1309 (1975); M. Duong-van, K. V. Vasavada and R. Blankenbecler, Phys. Rev. D16, 1389 (1977).

6. For a recent review of the conventional QCD approach, see A. J. Buras, Fermilab Report PUB-79/17-THY.

7. W. E. Caswell, R. R. Horgan and S. J. Brodsky, Phys. Rev. D18, 2415 (1978).

8. A detailed discussion is presented by S. J. Brodsky and G. P. Lepage, SLAC Reports SLAC-PUB-229 SLAC-PUB-2343 and SLAC-PUB-2348.

9. E. L. Berger, J. Donohue and S. Wolfram, Phys. Rev. D17, 858 (1978); J. Donohue in Phenomenology of Quantum Chromodynamics, Rencontre de Moriond, 1978, ed. by J. Tran Thanh Van, Vol. I, p. 159; E. L. Berger in New Results in High Energy Physics - 1978, Vanderbilt Conference, ed. by R. S. Panvini and S. E. Csorna, p. 178; J. C. Collins and D. E. Soper, Phys. Rev. D16, 2219 (1977).

10. K. Kajantie, J. Lindfors and R. Raitio, Phys. Lett. 74B, 384 (1978); J. Cleymans and M. Kuroda, Phys. Lett. 80B, 385 (1979); J. C. Collins, Phys. Rev. Lett. 42, 291 (1979).

11. Chicago-Princeton Collaboration, C. B. Newman et al., Phys. Rev. Lett. 42, 951 (1979); G. E. Hogan et al., Phys. Rev. Lett. 42, 948 (1979); and K. J. Anderson et al., Phys. Rev. Lett. 42, 944 (1979).

12. S. D. Drell, D. J. Levy and T. M. Yan, Phys. Rev. D1, 1617 (1970); J. D. Sullivan, SLAC Topical Conference on Deep Inelastic Electroproduction, 1973, SLAC Report-167, Vol. 1. For a discussion of non-Born diagrams, see P. V. Landshoff and J. C. Polkinghorne, Phys. Rev. D6, 3708 (1972).

13. I. Schmidt and R. Blankenbecler, Phys. Rev. D16, 1318 (1977); I. Schmidt, SLAC Report-203, Ph.D. Thesis submitted to Stanford University (1977); A. Fernandez-Pacheco, J. A. Grifols and I. A. Schmidt, Lett. Nuovo Cimento 22, 339 (1978).

14. L. F. Abbott, E. L. Berger, R. Blankenbecler and G. L. Kane, SLAC Report SLAC-PUB-2327, and references therein.

15. R. D. Field and R. P. Feynman, Phys. Rev. D15, 2590 (1977).

16. H. Georgi and H. D. Politzer, Phys. Rev. Lett. 40, 3 (1978).

17. R. N. Cahn, Phys. Lett. 78B, 269 (1978).

18. See the review by G. Hanson, SLAC Report SLAC-PUB-2118; G. Hanson et al., Phys. Rev. Lett. 35, 1609 (1975).

19. M. Jacob and P. Landshoff, Phys. Reports 48, 285 (1978).

20. S. D. Drell and T. D. Lee, Phys. Rev. D5, 1738 (1972).

21. M. D. Mestayer, SLAC Report-214 (August, 1978), Ph.D. Dissertation.

22. L. F. Abbott and R. M. Barnett, SLAC Report SLAC-PUB-2375 (1979).

FIGURE CAPTIONS

1. (a) [illegible] quark is removed from an incident π [illegible] N. The quark carries four momentum p_1.

   (b) The shaded oval represents the full wave function for pion dissociation into an [illegible] upper line marked with an [illegible] and an off-shell quark p_a carrying four momentum squared p_a^2. In the large p_a^2 limit, the large momentum behavior of the full wave function can be represented by single gluon exchange, as sketched on the right-hand side of (b). The unshaded oval stands for the pion wave function at small momentum, where all lines are essentially on-shell.

2. Diagrams for $\pi q \to \gamma^* q$, $\gamma^* \to \mu^+\mu^-$. Solid single lines represent quarks. Symbols p_1, p_a, p_b and p_c denote four-momenta of quarks, and k is the four-momentum of the gluon.

3. Results from the Chicago-Princeton collaboration (Ref. 4) on the variation of the distribution $d\sigma/d\cos\theta$ with x_a in $\pi^- N \to \mu\bar{\mu}X$ at 225 GeV/c. Curves drawn through the data points are fits to the form $[1 + \alpha\cos^2\theta]$.

4. Polarization parameter α as a function of x_a for $\pi^- N \to \mu\bar{\mu}X$ at 225 GeV/c. The curve is a prediction of the model discussed in the text. Data are from Ref. 4.

5. (a) Sketch of $\ell N \to \ell' \pi X$; Q labels the exchanged γ^* or W. The intermediate quark labeled p_a is off-shell and timelike. The initial quark from the incident nucleon carries four momentum xp_N.

   (b) On the left is a diagram showing the dissociation of an off-shell virtual quark into a pion plus X. The shaded oval

represents the full behavior of this amplitude. At large squared four-momentum p_a^2 where $p_a^2 \propto p_T^2/(1-z)$, the large momentum behavior of the dissociation amplitude may be represented by the single gluon exchange diagram sketched on the right, in which the quark lines marked with crosses (×) are essentially on-shell.

6. Gauge-invariant set of diagrams for $\ell N \to \ell' \pi X$; k labels the four-momentum of the exchanged gluon. Solid lines, except for the ones labeled π, z and ℓ', are quark lines.

7. Gauge-invariant set of diagrams for $e^+e^- \to \pi X$.

8. Predicted behavior of the polarization parameter α as a function of z for $e^+e^- \to \pi X$ at two values of the center of mass energy.

9. One of the gauge-invariant set of diagrams for $h_1h_2 \to \pi X$, via the subprocess $qq \to \pi qq$. Here Q and k label the four-momenta of gluon exchanges, and p_a denotes the off-shell quark.

10. Diagrams illustrating the coupling of a photon to one of the three quark lines in the nucleon. In (a), gluons are exchanged between the three quark lines. In (b) and (c), two of the quarks are paired in a diquark system. In (b), the photon is coupled to the bachelor quark, whereas in (c), it couples to the diquark.

11. Figure taken from Ref. 14 showing $R(x,Q^2) = \sigma_L/\sigma_T$ for $ep \to e'X$ as a function of x for six values of Q^2. The solid line is obtained from the diquark model proposed in Ref. 14. The data are from Ref. 21.

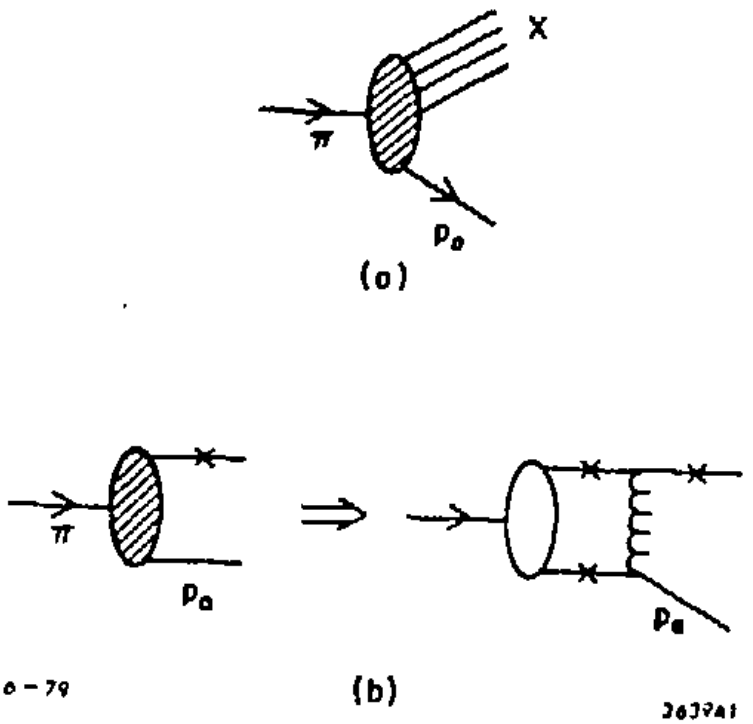

Fig. 1

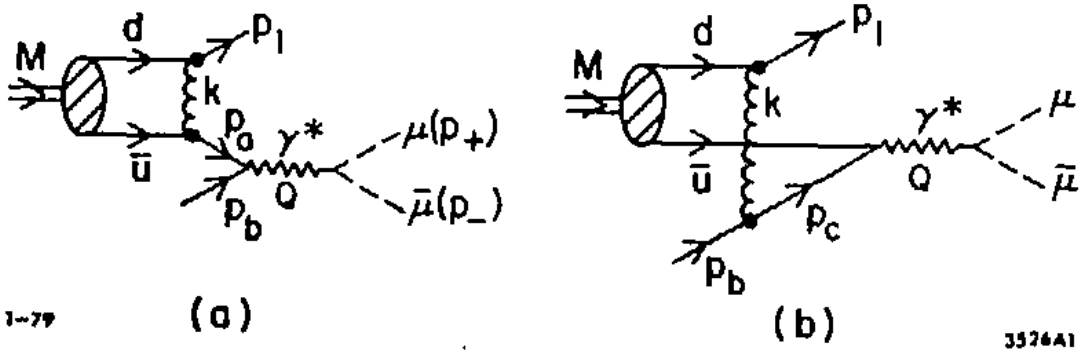
M
d
p_1
k
p_a
γ^*
$\mu(p_+)$
$\bar{u}$
Q
$\bar{\mu}(p_-)$
p_b
1-79
(a)
M
d
p_1
k
γ^*
μ
$\bar{u}$
Q
$\bar{\mu}$
p_c
p_b
(b)
3526A1

Fig. 2

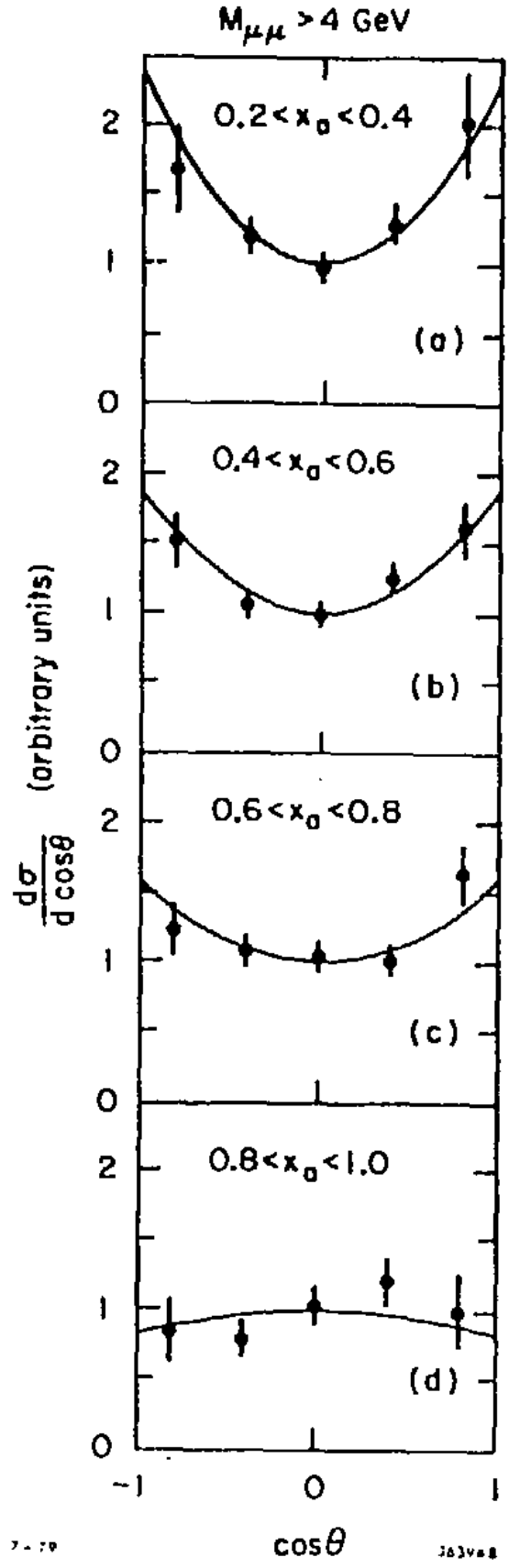
$M_{\mu\mu} > 4$ GeV
$0.2 < x_a < 0.4$
(a)
$0.4 < x_a < 0.6$
(b)
$0.6 < x_a < 0.8$
(c)
$0.8 < x_a < 1.0$
(d)
$\frac{d\sigma}{d\cos\theta}$ (arbitrary units)
$\cos\theta$
0
1
2
−1

Fig. 3

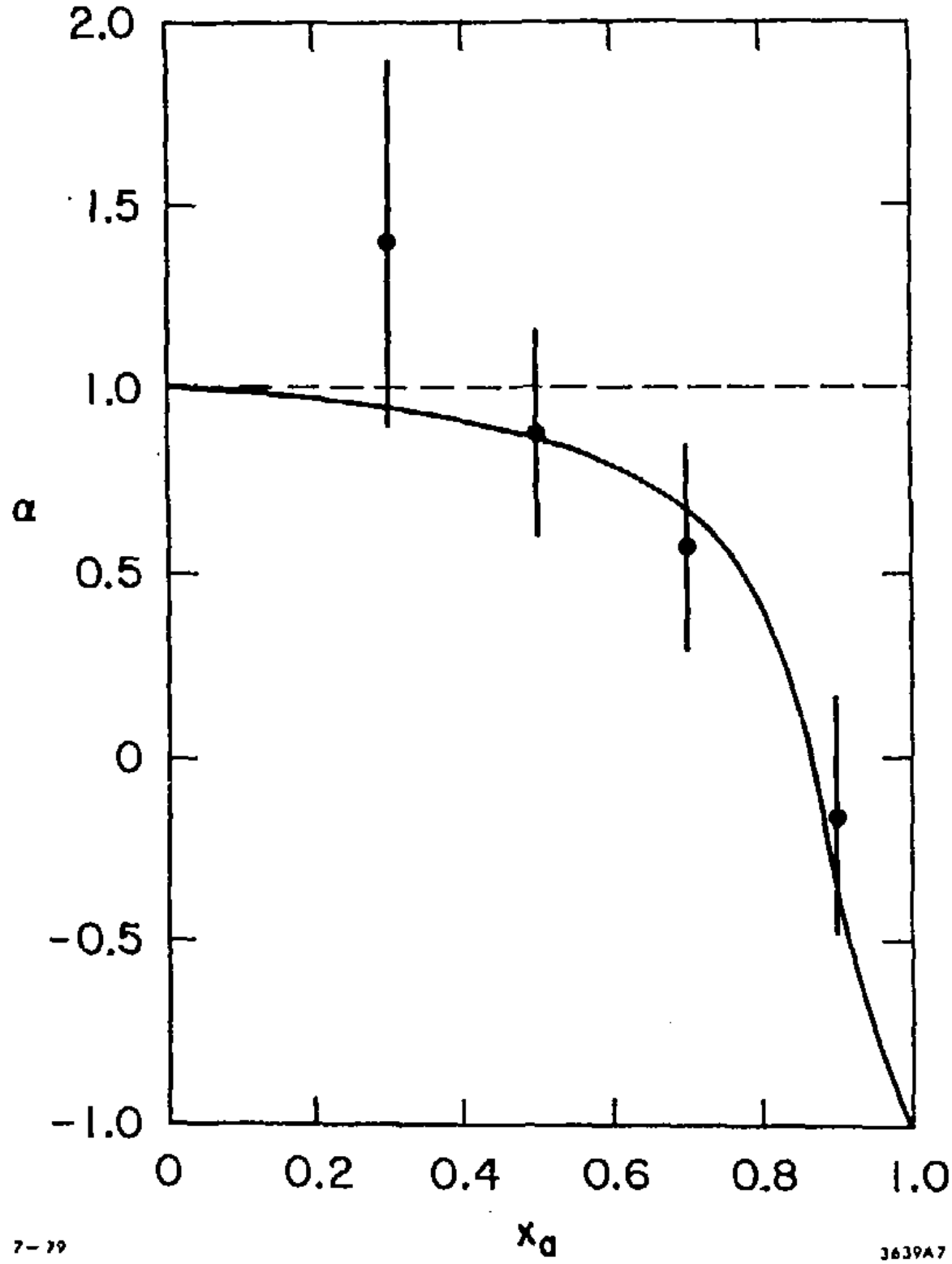

Fig. 4

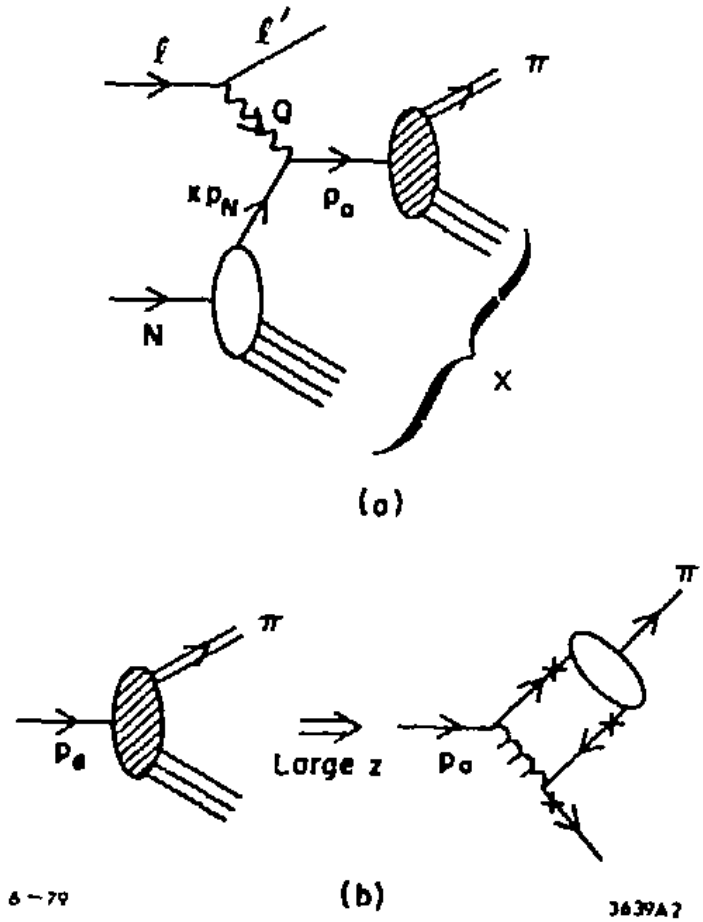

Fig. 5

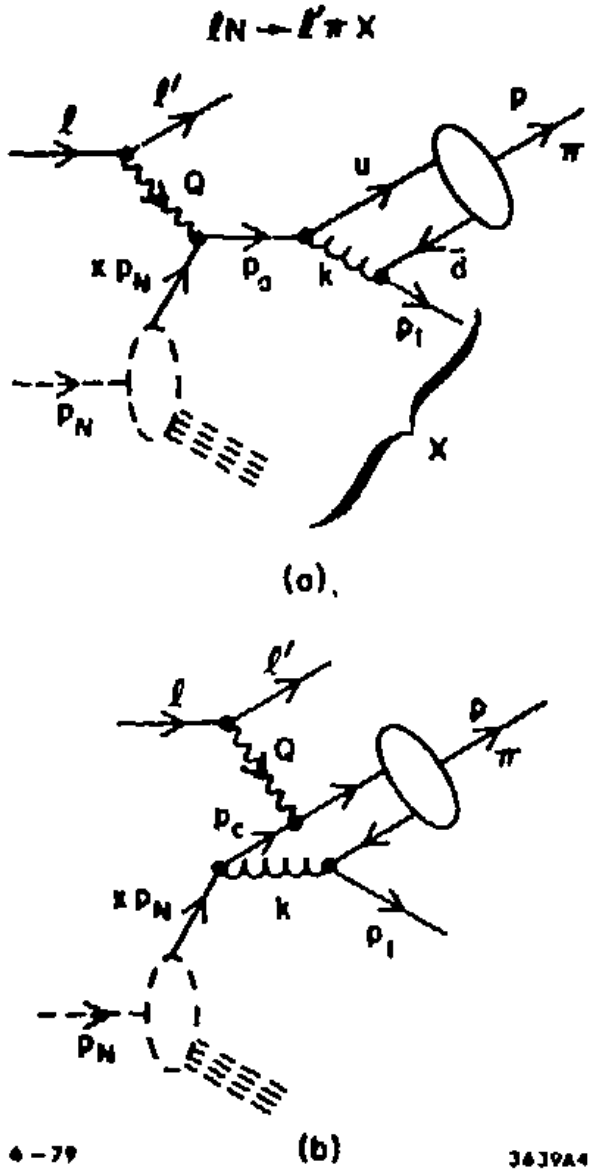

Fig. 6

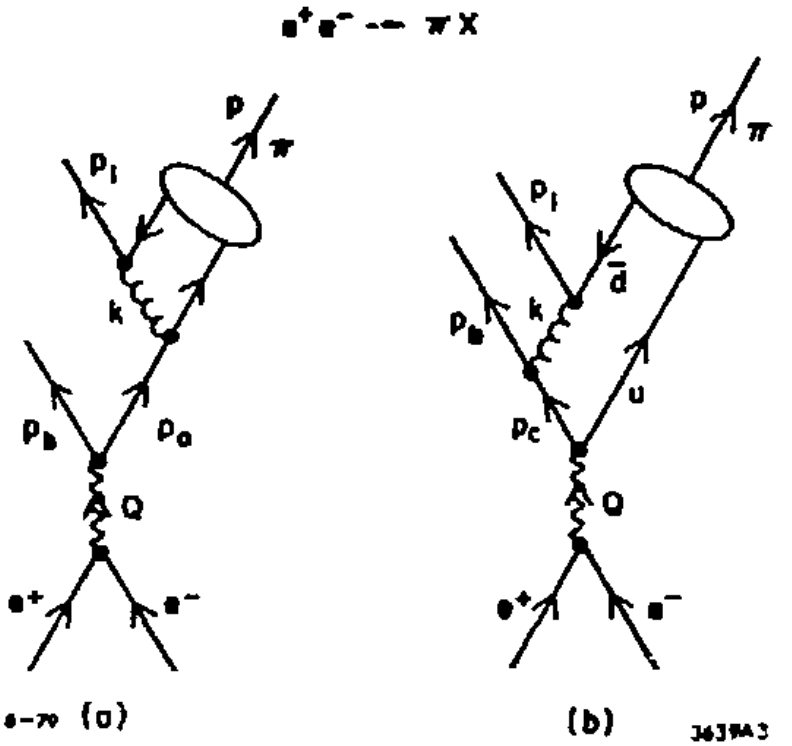

Fig. 7

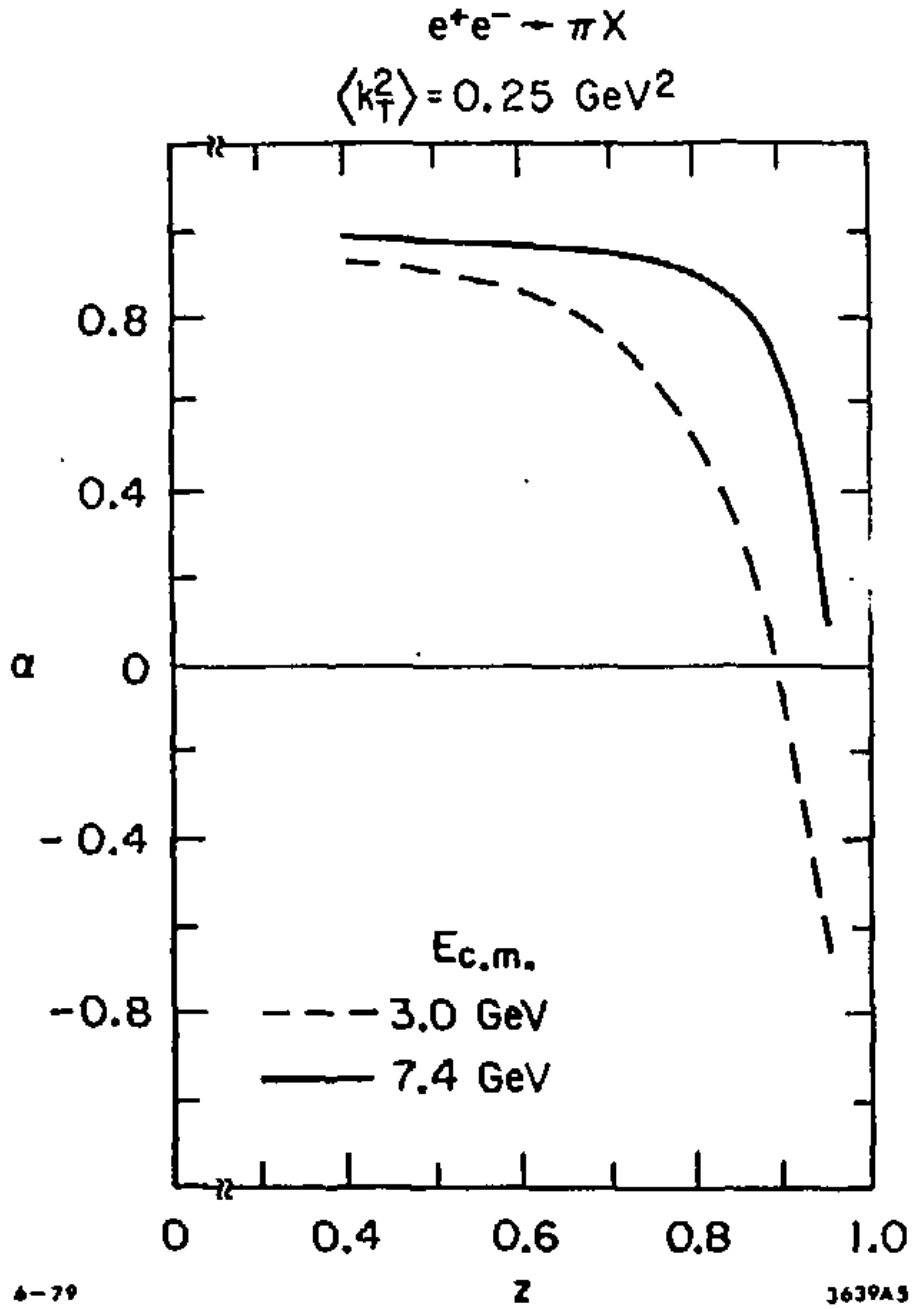
$e^+e^- \to \pi X$
$\langle k_T^2 \rangle = 0.25$ GeV^2
0.8
0.4
α
0
-0.4
-0.8
$E_{c.m.}$
3.0 GeV
7.4 GeV
0
0.4
0.6
0.8
1.0
z
6-79
3639A5

Fig. 8

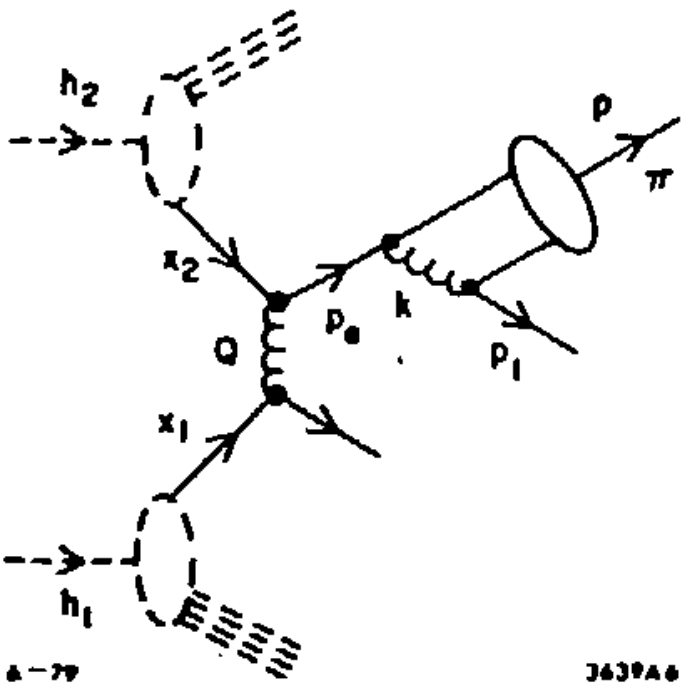

Fig. 9

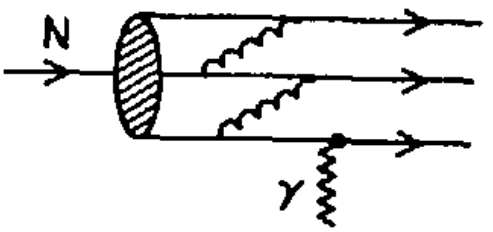

(a)

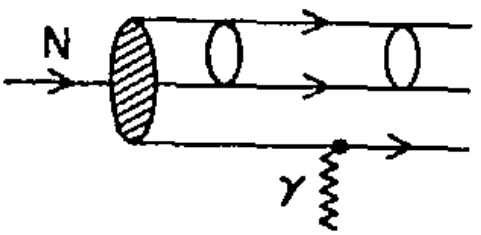

7-79 (b)

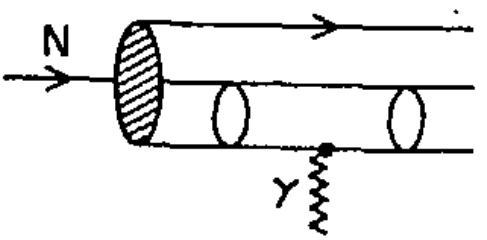

(c) 3639A9

Fig. 10

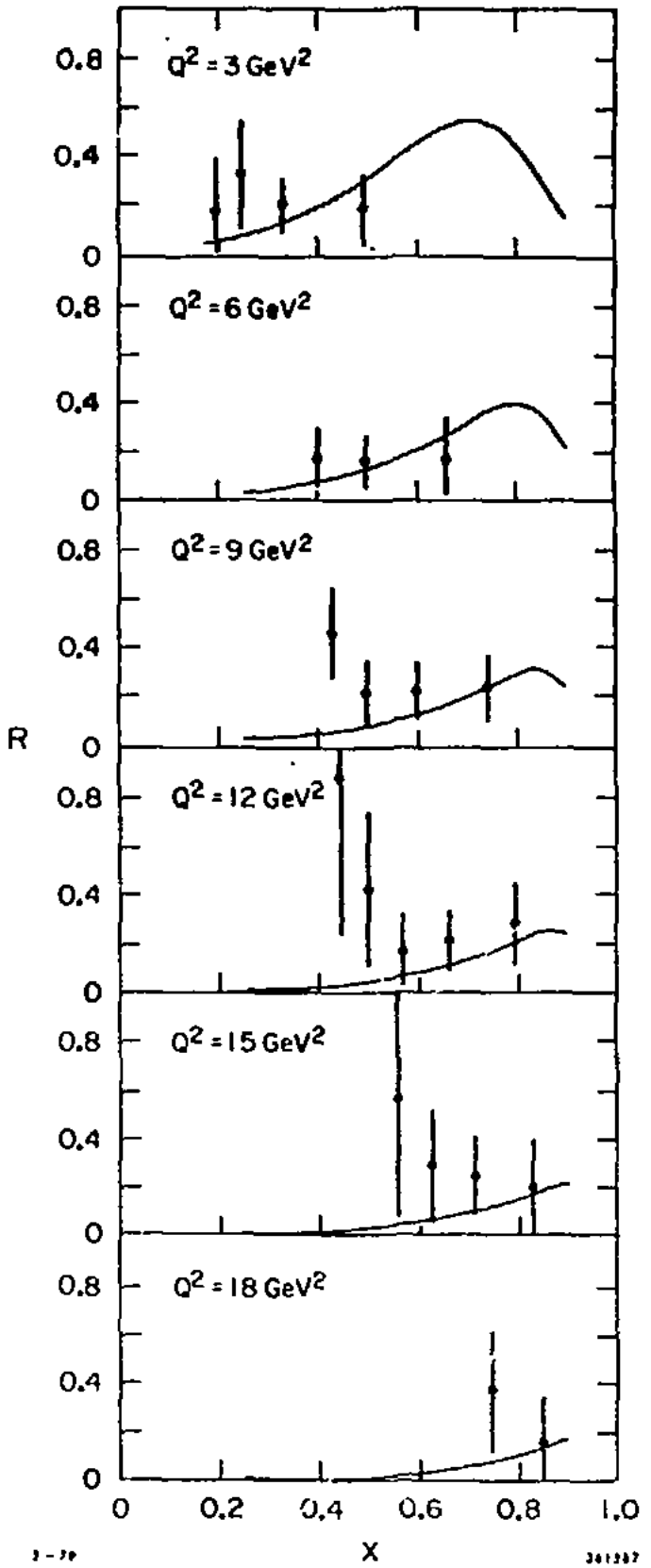
$Q^2 = 3\ GeV^2$
$Q^2 = 6\ GeV^2$
$Q^2 = 9\ GeV^2$
$Q^2 = 12\ GeV^2$
$Q^2 = 15\ GeV^2$
$Q^2 = 18\ GeV^2$
R
X
0
0.2
0.4
0.6
0.8
1.0

Fig. 11